Controlling bistability in microelectromechanical resonators

Qingfei Chen and Liang Huang
Department of Electrical Engineering, Arizona State University, Tempe, Arizona 85287, USA

Ying-Cheng Lai
Department of Electrical Engineering and Department of Physics and Astronomy, Arizona State University, Tempe, Arizona 85287, USA

For a microelectromechanical (MEM) resonator, the combination of mechanical nonlinearity and electrical driving force can lead to bistability. In such a case, the system exhibits two coexisting stable oscillatory states (attractors): one with low and another with high energy. Under the influence of noise, with high probability the system can be perturbed into the low-energy state. We propose a robust control scheme to place the system in the high-energy state. Our idea is not to pull the system out of the bistable regime but instead to take advantage of the nonlinear dynamics to achieve high-energy output. In particular, our control scheme consists of two steps: bifurcation control that temporarily drives the system to a regime with only one attractor, one that is the continuation of the high-energy attractor in the bistable regime; and ramping parameter control that restores the bistability while maintaining the system in the high-energy attractor. We derive an analytic theory to guide the control, provide numerical examples, and suggest a practical method to realize the control experimentally. Our result may find potential usage in devices based on MEM resonators where high output energy is desired. © *2008 American Institute of Physics*. [DOI: 10.1063/1.2825598]

Small-sized devices such as microelectromechanical systems (MEMS) and nanoelectromechanical systems have become common in many fields of science and engineering.[1–7] These devices have a simple structure but they show surprisingly rich dynamical behaviors such as bistability, chaos, and energy localization. A main challenge in applications of small-sized devices is how to achieve high output energy. This is important for practical devices such as resonators and microgenerators. One way to address this problem is to use large arrays of coupled MEMS resonators to obtain large output.[6] However, there are potential difficulties to employ this scheme in realistic applications due to the many complex and undesirable dynamical behaviors associated with it, such as energy localization[7] and spatiotemporal chaos.[8] An alternative approach is to use a strong driving force to enhance the oscillating energy of the MEM beam. In such a case, a common obstacle to high-amplitude oscillation is bistability, where two stable states coexist: one of high and another of low amplitude. There is usually a high probability that the system dynamics approaches the low-energy state for random initial conditions. A remedy to overcome this difficulty is to use control to stabilize the system in a high-energy oscillation mode. In this paper, we develop a robust control scheme to achieve this goal. In particular, we investigate a MEM cantilever-beam resonator, perhaps the most common element in MEM devices. Assuming that the system is in a bistable regime, we articulate a control strategy that consists of two steps: bifurcation control to place the system in the vicinity of an attractor that is the continuation of the high-energy mode in the bistable regime, and ramping parameter control to bring the system back to the original parameter regime while maintaining the high-energy oscillations.

The controls are guided by analytic formulae that we obtain using the averaging method. We also suggest an experimental implementation of the control strategy. Our work provides a well justified and practically viable approach to achieving desirable performance from MEM resonators.

I. INTRODUCTION

Microelectromechanical (MEM) resonators in the form of cantilever or doubly clamped beams have attracted a great deal of attention in recent years.[1–6] These resonators are the core of many MEM based, state-of-the-art technologies. While the small sizes of MEM resonators can bring significant benefits in a variety of applications, such as microgenerators, the outputs of such resonators are accordingly small, which may lead to low sensitivity, for example, in a sensor application. This can degrade the system performance when electrical and/or mechanical noise is present. It is thus of interest to investigate viable approaches to enhancing the output energies of MEM resonators. In basic physics, the dynamics of MEM oscillators are also of great interest. For instance, an array of coupled MEM cantilever beams can exhibit the phenomenon of energy localization,[7] which is ubiquitous in many other systems in condensed matter and optical physics.[9] Due to its accessibility to high-precision and demanding experimental studies, MEM oscillator arrays have become a paradigm for understanding the energy-localization phenomenon in complex physical systems.[9] In order to achieve large energy output from a MEM resonator, its key component, typically a cantilever beam, needs to oscillate with a large amplitude. One may attempt to address the problem by searching for better materials. However,

there are limits to material properties.[10] An alternative approach is to employ a strong background driving force to enhance the oscillation of the MEM beam. This approach is feasible if the underlying system is linear, where a high input would correspondingly generate a high output. The difficulty is that a MEM beam system, when subject to strong external forcing, typically behaves nonlinearly.[1–6] For a nonlinear dynamical system, strong input can result in low output that cannot possibly meet the energy requirement. In this regard, for a MEM beam resonator the most common obstacle to high-amplitude oscillation is bistability, where the system exhibits two stable states (attractors): one of high and another of low amplitude. For a randomly prepared initial state, there is a high probability that the system dynamics approaches the low-amplitude state. This is so because, if the initial energy of the system is low, its dynamical state will be in the basin of the low-energy attractor. Even when the system is initially in a high-energy state, random parameter drift, noise, and external perturbations can all move the system into the low-amplitude state. To achieve certain desired energy output, a control strategy is necessary.

In this paper, we develop an effective control method to maintain a MEM beam resonator in its high-energy state. Assume the system operates in a bistable regime so that high-amplitude oscillations are one of the allowed states of the system. Our idea is based on *bifurcation control* to perturb the system by changing an accessible parameter so that it is in a regime where only one attractor exists, which is the continuation of the high-energy attractor in the bistable regime. The parameter is then changed gradually back to its original value in a way so as to keep the system in the vicinity of the high-amplitude attractor. We call this step *ramping parameter control*. To demonstrate the working of our control method, we shall consider a simplified model of MEM cantilever beam and obtain analytic understanding of the bifurcation of the system by using the averaging method (Sec. II). A control law can then be derived based on the analytic formula and numerical demonstration will be provided (Sec. III). A possible scheme for experimental implementation of our control method will be proposed (Sec. IV).

II. BIFURCATION ANALYSIS

The dynamics of a MEM cantilever beam is in general described by a sophisticated nonlinear partial differential equation[3] that involves complicated mechanical and electrical interactions between the beam and its surroundings. However, if one focuses on the motion of the free end of the beam, the system equation can be simplified greatly as the following nonlinear ordinary differential equation:[11]

$$m\ddot{x} + b\dot{x} + k_2 x + k_4 x^3 = m\alpha \cos(2\pi f t), \quad (1)$$

where m is the equivalent mass of the beam, $x(t)$ is the displacement of the beam's free end, b is the damping coefficient, k_2 and k_4 are the harmonic and quadratic spring constants, respectively. The sinusoidal driving force term of the amplitude $m\alpha$ (α is the acceleration) and frequency f come from the interaction of the beam with an external time-varying electrical field. If α is large, the frequency response

of the beam will be strongly nonlinear, typically exhibiting bistability. To obtain an analytic understanding of the dynamical behavior of the system, we make use of the averaging method.[14] In particular, we write $x(t) = U(t)\cos(\Omega t) + V(t)\sin(\Omega t)$, where $\Omega = 2\pi f$ is the angular velocity of the driving, $U(t)$ and $V(t)$ are sinusoidal amplitude-modulating functions. Let $u(t)$ and $v(t)$ be the averaged functions of $U(t)$ and $V(t)$, respectively, over one driving period $T = 2\pi/\Omega$. We obtain, from Eq. (1), the following set of two coupled equations:[14]

$$\frac{du}{dt} = (\Omega^2 - \Omega_0^2)v - \frac{3}{4}\frac{k_4}{m}v(u^2 + v^2) + \frac{\Omega_0}{Q}\Omega u,$$

$$\frac{dv}{dt} = (\Omega^2 - \Omega_0^2)u - \frac{3}{4}\frac{k_4}{m}u(u^2 + v^2) - \frac{\Omega_0}{Q}\Omega v + \alpha, \quad (2)$$

where $\Omega_0 = \sqrt{k_2/m}$ is the intrinsic linear frequency of the beam and $Q = \sqrt{mk_2}/b$ is the quality factor of the beam. The average amplitude function is $H(t) = \sqrt{u^2(t) + v^2(t)}$, and from Eq. (2), we obtain

$$\left\{ \left[(\Omega_0^2 - \Omega^2) - \frac{3}{4}\frac{k_4}{m}H \right]^2 + \frac{\Omega^2 \Omega_0^2}{Q^2} \right\} H = \alpha^2. \quad (3)$$

It can be seen that if $k_4 = 0$, Eq. (3) represents the standard linear frequency response equation. Note that the model equations are not made dimensionless so that comparison with experimental results is convenient. In particular, to illustrate the occurrence of bistability, we set the following parameter values: $(m, b, k_2, k_4, f, \alpha) = (5.46 \times 10^{-13}$ kg, 6.24×10^{-11} kg/s, 0.303 N/m, 5×10^8 N/m^3, 1.25×10^5 Hz, 1.56×10^4 m/s^2), which are chosen based on the experimental MEM cantilever beam in Ref. 7. For relatively small value of the driving acceleration α, the frequency response is similar to that from a linear system, as shown by the lower curve in Fig. 1. As α is increased, bistability gets in, causing the frequency response to be nonlinear, as shown by the upper trace in Fig. 1, where the two vertical lines denote the boundaries of the bistable regime in which there are two stable solutions, one of relatively large amplitude and another of smaller amplitude, and an unstable solution (dashed curve) in between the stable solutions. In the bistable regime, the frequency response thus exhibits a hysteresis behavior. Dynamically, bistability is induced by saddle-node bifurcations of the system as α is varied. At the lower-frequency boundary, the stable solution with large amplitude is continuous, and the low-amplitude solution is generated by a saddle-node bifurcation. Likewise, the saddle-node bifurcation that creates the high-amplitude solution occurs at the upper-frequency boundary of the bistable regime, at which the lower-amplitude solution is continuous. We observe that for given parameter values, oscillations of large amplitude occurs in the bistable regime. Our goal is to stabilize the system in the large-amplitude state.

Suppose now the system is in the bistable regime. Without control, there is a high probability that the system will be in the low-amplitude state. In order to achieve high output energy, it is necessary to "place" the system at the high-amplitude branch. One way to achieve this is to apply control

to shift the bistable regime toward large frequencies so that, when the driving frequency is fixed, the system gets out of the bistable regime and is in a regime where the high-amplitude state is the only stable solution (bifurcation control). To guide the bifurcation control, it is necessary to pre-

dict the saddle-node bifurcation at the lower-frequency boundary of the bistable regime. In the following, we derive an analytic formula for this bifurcation point.

The Jacobian matrix of system (2) at its fixed point $X=(u,v)$ is

$$\mathbf{DF(X)} = \frac{1}{2\Omega} \begin{pmatrix} -\dfrac{\Omega_0\Omega}{Q} + \dfrac{3k_4uv}{2m} & -(\Omega^2 - \Omega_0^2) + \dfrac{3k_4(u^2 + 3v^2)}{4m} \\ \Omega^2 - \Omega_0^2 - \dfrac{3k_4(3u^2 + v^2)}{4m} & -\dfrac{\Omega_0\Omega}{Q} - \dfrac{3k_4uv}{2m} \end{pmatrix}. \tag{4}$$

Denote the two eigenvalues of $\mathbf{DF(X)}$ as λ_1 and λ_2, respectively. At a saddle-node bifurcation point, at least one of these two eigenvalues is zero. Thus, a criterion for saddle-node bifurcation is

$$\begin{aligned}
\lambda_1\lambda_2 &= |\mathbf{DF(X)}| \\
&= \frac{1}{4\Omega^2}\left(\frac{\Omega_0^2\Omega^2}{Q^2} + (\Omega^2 - \Omega_0^2) - \frac{3k_4}{m}(\Omega^2 - \Omega_0^2)(u^2 + v^2) \right. \\
&\quad \left. + \frac{27k_4^2}{16m^2}(u^2 + v^2)^2 \right) = 0,
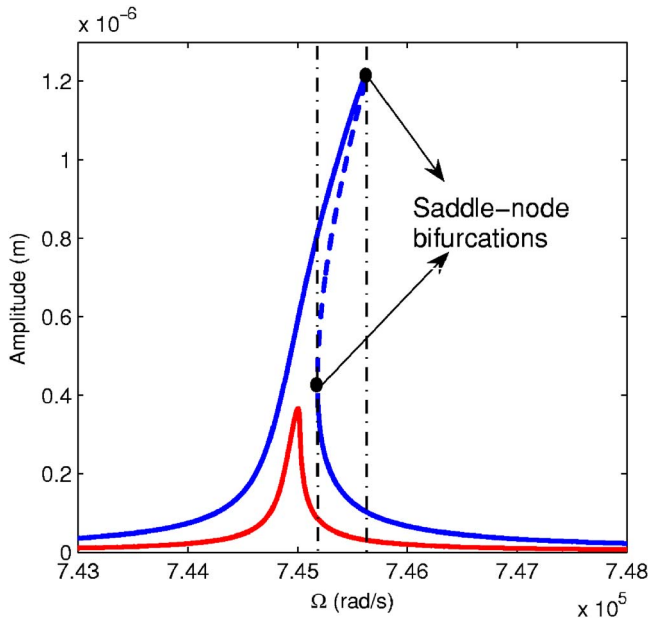\end{aligned} \tag{5}$$

which gives

FIG. 1. (Color online) Response amplitude as a function, obtained from Eq. (3), of the frequency Ω. Solid curves are stable solutions and the dashed curve indicates an unstable solution. The driving acceleration is $\alpha = 31.2$ m/s^2 for the lower line and $\alpha = 104$ m/s^2 for the upper line. The left vertical line is from theory [Eq. (11)].

$$\frac{\Omega_0^2\Omega^2}{Q^2} + (\Omega^2 - \Omega_0^2) - \frac{3k_4}{m}(\Omega^2 - \Omega_0^2)H + \frac{27k_4^2}{16m^2}H^2 = 0. \tag{6}$$

Substituting Eq. (6) into Eq. (3), we obtain

$$H^3 - \frac{4m}{3k_4}(\Omega^2 - \Omega_0^2)H^2 - \frac{8m^2\alpha^2}{9k_4^2} = 0. \tag{7}$$

Denoting $p = -4m(\Omega^2 - \Omega_0^2)/(3k_4)$, $q = 0$, $r = -8m^2\alpha^2/(9k_4^2)$. We can express Eq. (7) as $H^3 + pH^2 + qH + r = 0$. The cubic roots of Eq. (7) can be written as

$$H_1 = p/3 + A + B,$$
$$H_{2,3} = p/3 - (A + B)/2 \pm (A - B)\sqrt{-3}/2, \tag{8}$$

where

$$A = \sqrt[3]{\sqrt{M^2 + N^3} - M}, \quad B = b\sqrt[3]{-\sqrt{M^2 + N^3} - M},$$

$$M = (2p^3 - 9pq + 27r)/54, \quad N = (3q - p^2)/9.$$

At the saddle-node bifurcation, one of the stable fixed points coalesces with the unstable fixed point so that there are only two roots of Eq. (7) at the bifurcation point. Thus, a necessary condition for saddle-node bifurcation is

$$M^2 + N^3 = [(2p^3 - 9pq + 27r)/54]^2 + [(3q - p^2)/9]^3 = 0. \tag{9}$$

Since $q = 0$, we obtain

$$p^3 = -27/2r. \tag{10}$$

Utilizing the definitions of the quantities p, q, and r, we obtain the critical frequency (or resonant frequency) Ω_c at the bifurcation point,

$$\Omega_c = \sqrt{\frac{k_2}{m} + \frac{3}{2}\left(\frac{3k_4\alpha^2}{2m} \right)^{1/3}}. \tag{11}$$

For $\Omega < \Omega_c$, the system has one stable fixed point, but for $\Omega > \Omega_c$, there are two stable fixed points, as shown in Fig. 1. Equation (6) can also be derived by a perturbation method,[15] but the explicit form of Ω_c [Eq. (11)] is not given in this reference.

Figure 2 shows the numerically obtained value of the bifurcation point Ω_c as a function of the harmonic spring
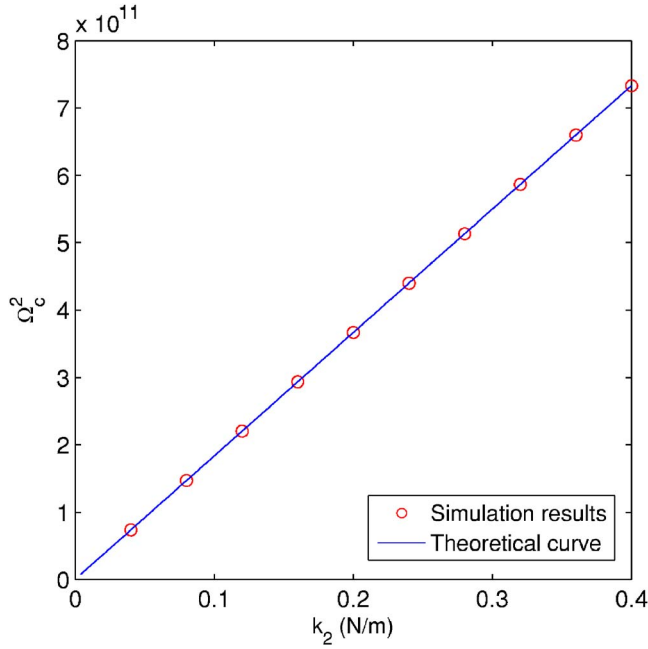
FIG. 2. (Color online) The square of the value of saddle-node bifurcation point Ω_c^2 as a function of the harmonic spring constant k_2. In the figure, $(m, b, k_4, \Omega, \alpha) = (5.46 \times 10^{-13}$ kg, 6.24×10^{-11} kg/s, 5×10^8 N/m^3, 7.85×10^5 rad/s, 1.56×10^4 m/s$^2)$. The solid line is the theoretical result from Eq. (11) and the circles are simulation results obtained by estimating the lower boundary of the bistable regime from the original system Eq. (1).

constant (open circles). They are obtained by estimating the lower boundaries of the bistable regime in driven system (1), as shown in Fig. 1. The solid line lying on top of the numerical points is from the theoretical prediction derived from Eq. (11): $\Omega_c^2 = k_2/m + 1.5(3k_4\alpha^2/(2m))^{1/3}$, in which Ω_c^2 and k_2 have a linear relationship. For the parameters used in simulation, the values of the first term in the square root of Eq. (11) range from $k_2/m = 8 \times 10^{10}$ to 5.55×10^{11}, and the second term is $1.5(3k_4\alpha^2/(2m))^{1/3} = 1.04 \times 10^{10}$. One can see that the nonlinearity of the beam can shift the resonant frequency, and for small k_2, the shift can be as large as 10%.

One feature of Eq. (11) is that Ω_c does not depend on the damping coefficient b. This indicates that the saddle-node bifurcation determining the lower boundary of the bistable regime is constant with respect to the variation of b. Since, for a MEM resonator, the damping is mostly due to the influence of the environment in which the cantilever beam is embedded, the independence of Ω_c on b suggests that any control scheme designed according to the saddle-node bifurcation approach be robust.

III. IMPLEMENTATION OF CONTROL

The goal of our control scheme is to stabilize a MEM cantilever beam in a high-amplitude oscillation state, taking advantage of the nonlinear dynamics of the system, in particular bistability. To achieve this, we first choose the system parameters such that it is in a bistable regime. We then apply a control so that the system moves out of the bistable regime to a regime where there is one stable solution; i.e., the one that is the continuation of the high-amplitude solution in the

bistable regime. Referring to Fig. 1, we see that this can be achieved by "pushing" Ω_c, the lower saddle-node bifurcation point, toward the right. From Eq. (11), we see that a simple way to achieve this is to "enhance" the harmonic spring constant k_2 by an appropriate amount. In particular, we generate a quantity $k_e > 0$ and add it to k_2. This additional amount of the harmonic spring constant k_e can be realized electrically through a proper feedback scheme.[16] Suppose the system operates at frequency Ω. The amount k_e can be determined by requiring

$$\Omega_c^e = \sqrt{\frac{k_2 + k_e}{m} + \frac{3}{2}\left(\frac{3k_4\alpha^2}{4m}\right)^{1/3}} > \Omega. \quad (12)$$

In Sec. IV, we will discuss a practical scheme to realize this in realistic device applications. After the bifurcation control, the system settles in the high-amplitude oscillation state. In order to bring the system back to its original parameter setting while maintaining the high-energy operation, we can apply ramping parameter control by reducing k_e gradually to zero, which is necessary to keep the system in the basin of the high-energy state.

In the following subsections, we analyze the two steps of our control scheme: bifurcation control and ramping parameter control.

A. Bifurcation control

With the linear feedback control term $k_e x$, the controlled system can be written as

$$m\ddot{x} + b\dot{x} + (k_2 + k_e)x + k_4 x^3 = m\alpha \cos(2\pi f t). \quad (13)$$

Utilizing the averaging method, we can calculate the asymptotic oscillation amplitude of the system as a function of the controlled spring constant $k_2 + k_e$. A representative example is shown in Fig. 3. We observe a saddle-node bifurcation for $k_2 + k_e \approx 0.3315$ N/m. Beyond this point, the system possesses only one stable solution, the continuation of the high-amplitude solution in the bistable regime.

Equation (13) involves k_4, the aharmonic spring constant, which is relatively more difficult to measure, say, than the harmonic spring constant k_2[12,13] due to the difficulty to measure Ω_c accurately in realistic situations where noise is present. Here we derive a criterion to place the system in the high-energy state without explicit knowledge of k_4. Our idea is to make use of the phenomenon of resonance. In particular, if the aharmonic force is weak as compared with the harmonic force, the system can be regarded as having an approximate intrinsic frequency. When this frequency matches the external driving frequency, a resonance occurs, which can cause the system to oscillate with a maximally possible amplitude. To proceed, we note from Eq. (4) that the eigenvalues of the system satisfy

$$\lambda_1 + \lambda_2 = -\Omega_0/Q < 0. \quad (14)$$

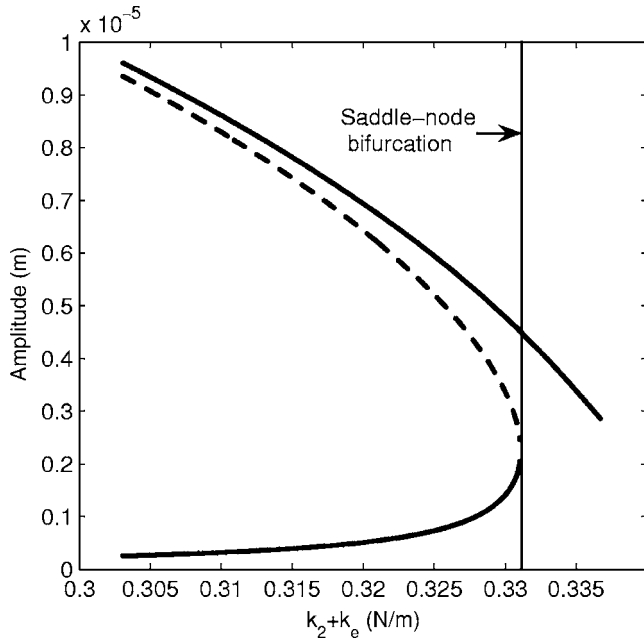Thus, at least one of the eigenvalues is negative. If $\Omega_0 = \Omega$, we have

FIG. 3. Response amplitude as a function of k_2+k_e. The solid curves are stable solutions and the dashed curve is unstable solution. In the figure, $\Omega = 7.85 \times 10^5$ rad/s and $k_4 = 5 \times 10^8$ N/m^3.
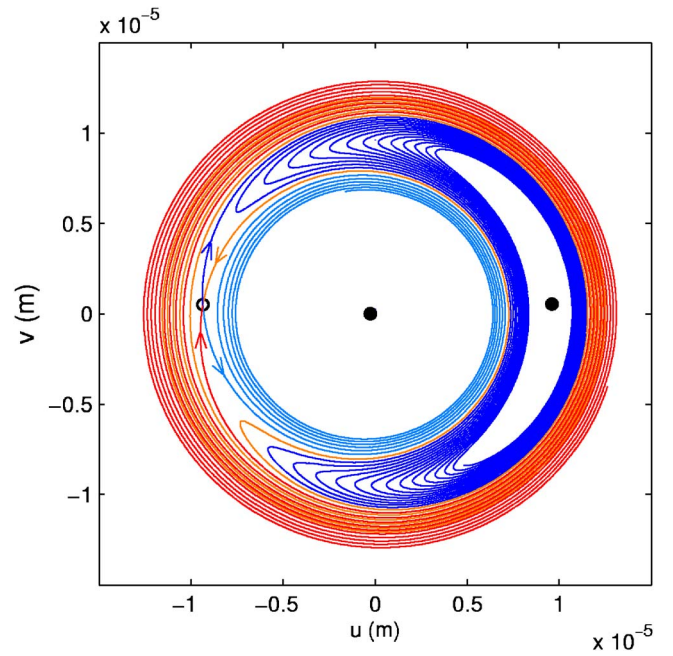

FIG. 4. (Color online) Stable and unstable manifolds of the saddle point in phase space. The parameters used in this figure are $(m, b, k_2, k_4, \Omega, \alpha) = (5.46 \times 10^{-13}$ kg, 6.24×10^{-11} kg/s, 0.303 N/m, 5×10^8 N/m^3, 7.85×10^5 Hz, 1.56×10^4 m/s^2), which are the same as the ones given in Sec. II.

$$\lambda_1 \lambda_2 = |\mathbf{DF(X)}|$$

$$= \frac{1}{4\Omega^2} \left[\frac{\Omega_0^2 \Omega^2}{Q^2} + (\Omega^2 - \Omega_0^2) \right.$$

$$\left. - \frac{3k_4}{m}(\Omega^2 - \Omega_0^2)H + \frac{27k_4^2}{16m^2}H^2 \right]$$

$$= \frac{\Omega_0^2}{4Q^2} + \frac{27k_4^2}{64m^2\Omega_0^2}H^2 > 0. \tag{15}$$

Equations (14) and (15) imply that both eigenvalues be negative, indicating the lack of any unstable solution. That is, when resonance occurs ($\Omega_0 = \Omega$), the system is necessarily outside the bistable regime. The occurrence of resonance stipulates that the system be in the high-energy state. Thus, it is only necessary to change k_e to induce a resonance to place the system in the high-energy state.

To achieve an approximately linear resonance state, knowledge of the aharmonic spring constant k_4 is not necessary. That is, we can set $\Omega = \sqrt{(k_2+k_e)/m}$, which gives the required control perturbation to k_2,

$$k_e = \Omega^2 m - k_2. \tag{16}$$

B. Ramping parameter control

In the bistable regime, the system possesses two stable fixed-point attractors, one with high and the other with low energy, each with its own basin. As a parameter of the system changes, the system, which is already in the high-energy state via a proper bifurcation control, can move into the basin of the low-energy attractor. The purpose of ramping parameter control is to keep the system in the high-energy state.

Figure 4 shows, in the two-dimensional phase space (u, v), a typical structure of the averaged system in the

bistable regime, where the fixed point attractors are denoted by closed circles, and the unstable saddle fixed point by open circle. The stable and unstable manifolds of the unstable fixed point are also shown. In this planar system, the two stable fixed-point attractors are in the enclosures of the unstable manifold originated from different directions of the saddle-fixed point, and its stable manifold is the boundary separating the basins of the fixed-point attractors.[14] The locations of the fixed points and the basin boundary depend on the control parameter. After the bifurcation control, the system is in the vicinity of the attractor that is the continuation of the high-energy attractor in the bistable regime. This attractor is located at the star in Fig. 5. If the control is suddenly removed, i.e., we make the harmonic spring constant k_2 to change from $k_2^0 + k_e$ to k_2^0, where k_2^0 is the original uncontrolled harmonic spring constant, the system will move along the dashed trace in Fig. 5, which is in the basin of the low-energy attractor for k_2. However, if we reduce k_2 gradually from $k_2^0 + k_e$ to k_2^0, the high-energy attractor will move its location smoothly, so will the basin boundary. If the rate of the parameter change is not too large, the system will always have time to approach and stay in the vicinity of the high-energy attractor, despite its shift in the phase space. This behavior is shown by the solid trace in Fig. 5. We see that, after the parameter control, the system parameters have been set back to their original, uncontrolled values, but the system has been firmly placed in the high-energy attractor.

C. Simulation of control

To actually implement the control scheme, we first set $k_2 = k_2^0$. The control parameter k_2 is then set to $k_2 = k_2^0 + k_e$, where k_e is determined by Eq. (16) based on the consider-
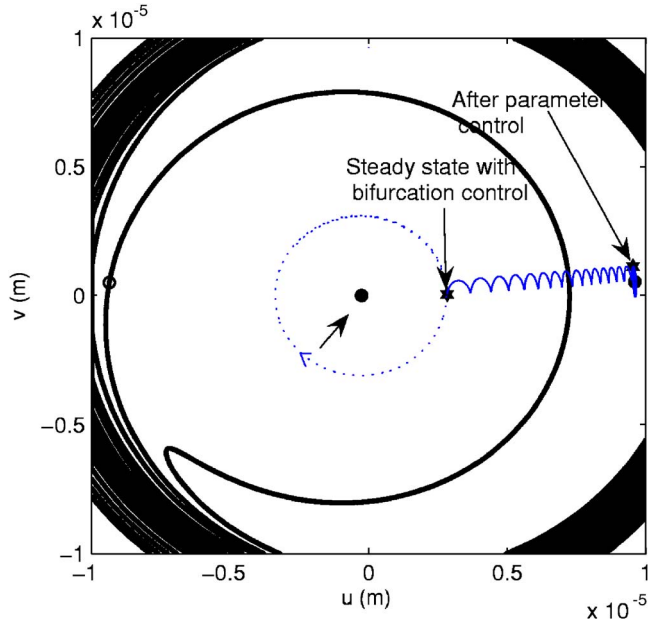
FIG. 5. (Color online) Dynamics of the system with (solid oscillating curve) and without (dashed circle) linearly decreasing parameter control. The thick line is the boundary of the basins of attraction for the two stable fixed points in the uncontrolled system for $k_2 = 0.303$ N/m.

ation of resonance. For our parameter setting, we obtain $k_e \approx 0.034$ N/m. The simulation result is shown in Fig. 6. Initially we have $k_2 = k_2^0$ and the system exhibits near-zero amplitude oscillation; i.e., it is in the vicinity of the low-energy attractor. Bifurcation control is applied at $t = 0.07$ s so that $\triangle k_2 \equiv k_2 - k_2^0$ is increased from zero to k_e, after which the system is in a regime where there is only one attractor, the continuation of the high-energy attractor. At $t = 0.14$ s, ramping parameter control begins, where $\triangle k_2$ starts to decrease gradually from k_2 to zero. We observe that, despite the pa-

rameter changes, the system oscillates with larger and larger amplitude, as it has been kept in the vicinity of the high-energy attractor, which moves further away from the lower boundary of the bistable regime as k_2 (or Ω_e) is reduced. As a result, the oscillation amplitude associated with the high-energy attractor keeps increasing as k_2 is reduced. At $t = 0.21$ s, ramping parameter control is ended, and the system parameters have been set back to their initial values before the control. Apparently, due to the control, the system oscillates with much larger amplitude, as shown in Fig. 6.

IV. DISCUSSION

In summary, we have devised a robust control scheme to allow a MEM cantilever beam to oscillate with a much larger amplitude than that which would occur without control. The basic guideline is to take advantage of the nonlinear dynamics of the system, in particular bistable frequency response. The system is first brought into an operational regime via some proper bifurcation control where the only attractor state is one that can be continued to the state with much higher energy in the bistable regime. The amount of parameter change necessary for the bifurcation control has been obtained analytically. Ramping parameter control is then applied to bring the system back to the bistable regime, but the system is maintained in the large-amplitude oscillation state. Since the high-energy state is associated with a fixed-point attractor in the phase space, small noise will not affect the control as, throughout the control, the system is always in the vicinity of the attractor, which is reasonably distant from the basin boundary. Our control scheme is thus expected to be robust and can be applied in realistic device application.

The central technical approach to realizing our control scheme is to modulate the harmonic spring constant of the MEM cantilever beam. Here we suggest a method that is potentially experimentally implementable. Say we fabricate a thin beam that is vertically attached to the resonant cantilever beam and then apply an electrostatic force through an electrode, the magnitude of which is determined by the voltage difference between the attached beam and the electrode. The instantaneous displacement $x(t)$ of the resonant cantilever beam can be measured by devices such as position-sensing circuit or optical microprobe.[17] The displacement is then fed into a properly designed circuit that provides a voltage signal proportional to the feedback control signal $k_e x(t)$, which then determines the desirable electrostatic force.
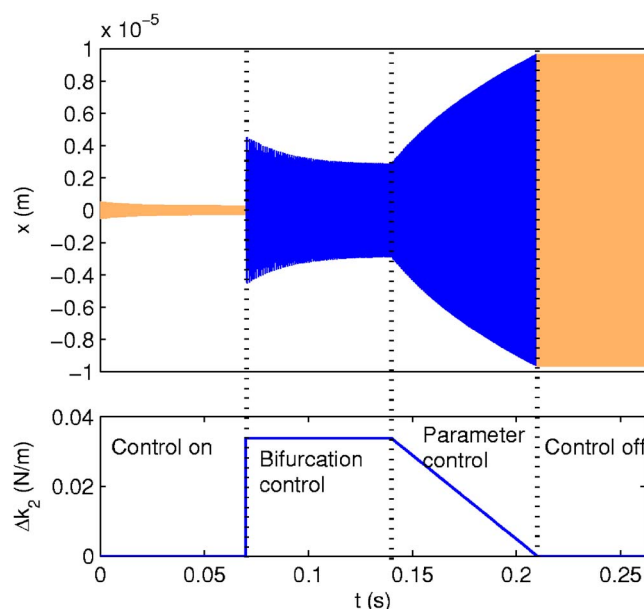
FIG. 6. (Color online) Simulation of the control in the driven system (1). The upper panel is the displacement x as a function of time and the lower panel is the control parameter $\Delta k_2 = k_e$ as a function of time.

[1]H. G. Craighead, Science **290**, 1532 (2000).
[2]X. M. H. Huang, C. A. Zorman, M. Mehregany, and M. L. Roukes, Nature (London) **321**, 496 (2003).
[3]S. K. De and N. R. Aluru, Phys. Rev. Lett. **94**, 204101 (2005).
[4]H. B. Peng, C. W. Chang, S. Aloni, T. D. Yuzvinsky, and A. Zettl, Phys. Rev. Lett. **97**, 087203 (2006).
[5]S.-B. Shim, M. Imboden, and P. Mohanty, Science **316**, 95 (2007).
[6]M. C. Cross, A. Zumdieck, R. Lifshitz, and J. L. Rogers, Phys. Rev. Lett. **93**, 224101 (2004).
[7]M. Sato, B. E. Hubbard, A. J. Sievers, B. Ilic, D. A. Czaplewski, and H. G.

Craighead, Phys. Rev. Lett. **90**, 044102 (2003).

[8]Q. Chen, L. Huang, and Y.-C. Lai (submitted).

[9]M. Sato, B. E. Hubbard, and A. J. Sievers, Rev. Mod. Phys. **78**, 137 (2006).

[10]R. Lifshitz and M. C. Cross, Phys. Rev. B **67**, 134302 (2003).

[11]P. Malatkar and A. H. Nayfeh, Nonlinear Dyn. **31**, 225 (2003).

[12]F. Ayela and T. Fournier, Meas. Sci. Technol. **9**, 1821 (1998).

[13]A. J. Dick, B. Balachandran, D. L. DeVoe, and C. D. Monte Jr., J. Micromech. Microeng. **16**, 1593 (2006).

[14]J. Guckenheimer and P. Holmes, *Nonlinear Oscillations, Dynamical Systems, and Bifurcations of Vector Fields, Applied Mathematical Sciences*, 3rd ed. (Springer, New York, 1990), Vol. 42.

[15]L. D. Landau and E. M. Lifshitz, *Course of Theoretical Physics I: Mechanics*, 3rd ed. (Pergamon, Oxford, 1976).

[16]G. T. A. Kovacs, *Micromachined Transducers Sourcebook* (McGraw-Hill, New York, 1998).

[17]J. M. Dawson, L. Wang, P. Famouri, and L. A. Hornak, Opt. Lett. **28**, 1263 (2003).